

PICOSECOND PHOTOMODULATION STUDY OF NANOCRYSTALLINE HYDROGENATED SILICON

M. Wraback, Lingrong Chen, J. Tauc and Z. Vardeny*

Brown University, Department of Physics and Division of Engineering,
Providence, Rhode Island 02912

*University of Utah, Department of Physics, Salt Lake City, Utah 84112

ABSTRACT

We have extended our photomodulation studies of nc-Si:H to the picosecond time domain. We measured the decays of photoinduced reflectivity with 100fs temporal resolution as a function of light intensity. Comparison with the data obtained on a-Si:H and c-Si indicates that ultrafast trapping and recombination processes are mainly the properties of the amorphous phase. It has also been observed that nc-Si:H is unstable under high illumination.

Introduction

We have applied the photomodulation (PM) spectroscopy to the study of electron states and carrier dynamics in nanocrystalline hydrogenated silicon (nc-Si:H). This technique employs two light sources: a pump beam for photogeneration of carriers, and a probe beam for measuring photoinduced changes in transmission and reflectivity. We have measured steady-state and time-resolved PM spectra in the time domain from 10^{-7} to 10^{-2} s, and have found that the data are compatible with the presence of two phases, amorphous and crystalline [1]. More recently we have employed the picosecond pump and probe technique to study ultrafast decays in reflectivity with a temporal resolution of 100fs. In this paper, we summarize the results on long time scales and present our new work in the picosecond regime, which provides information about ultrafast carrier trapping and recombination as well as photoinduced defects in nc-Si:H.

Experimental

The samples were nc-Si:H films 3-5 μ m thick deposited on crystalline Si substrates. They were prepared by the glow-discharge process in low-pressure hydrogen plasma in the floating potential condition with the substrate held at 300°C [1]. For the steady-state measurements the pump was a mechanically chopped cw Ar⁺ laser beam with an intensity of 100mW/cm² and the probe beam was derived from an incandescent lamp dispersed by a monochromator. The transient spectra with nanosecond resolution were measured on the system developed by Stoddart [2,3]. The pump pulse was obtained from a frequency-doubled Nd:YAG laser, and had a duration of 10ns, energy of 100 μ J, and repetition rate of 20s⁻¹. The diameter of the illuminated spot was about 1cm. The probe beam was produced with 0.1eV spectral resolution by an incandescent lamp and a set of interference filters of known transmission characteristics [2]. The transmission T and its photomodulation ΔT were recorded in the spectral range 0.25-1.8eV. In this range photoinduced changes in reflectivity can be neglected [4], and $-\Delta T/T = d\alpha$, where d is the film thickness and $\Delta\alpha$ is the change in the absorption coefficient α .

The light source for the low intensity picosecond experiments was a colliding pulse modelocked ring laser (CPM) [5], which produces 2eV optical pulses of 100fs duration and 0.1nJ pulse energy. These pulses were amplified to 2 μ J with a copper vapor laser pumped amplification stage [6] for the high intensity experiments. The beam was split into pump and probe pulses. Under high excitation conditions the pump pulse was focused to a diameter of 80 μ m

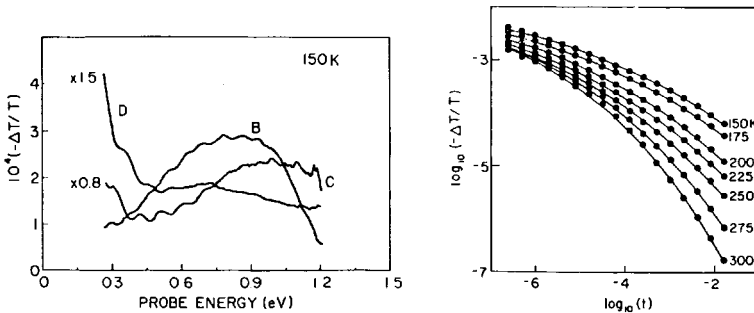


Fig. 1. Steady-state PM spectra of three samples--D, C, and B--at 150K: grain sizes are 830Å (sample D), 420Å (sample C), and 70Å (sample B).

Fig. 2 Measured PFCA decays of sample D using a probe energy of 0.25 eV at several temperatures. The fits (solid lines) are stretched exponentials.

on the sample. The probe pulse was delayed using a translation stage and focused inside the pump area to ensure the probing of a uniform carrier density. For the low excitation measurements both pump and probe pulses were focused to 25 μ m. In both cases the pump-induced change in reflectivity ΔR as measured by the modulation of the probe pulse was recorded as a function of the delay time between the probe and the pump pulses.

Steady-State and Transient Spectra

The steady-state PM spectra of three nc-Si:H films with crystallite grain sizes of 70Å (sample B), 420Å (sample C), and 830Å (sample D) at temperature $\theta = 150$ K are shown in Fig. 1 [1,7]. The spectrum obtained for sample B is similar to that of a-Si:H [8], with an onset of photoinduced absorption (PA) at about 0.5eV followed by photoinduced bleaching (PB) at about 1.0eV. In sample D this PM band is very weak, but there is a very strong onset of photoinduced absorption at low energies not found in sample B or a-Si:H. This long wavelength absorption has a frequency dependence of approximately ω^{-2} and is ascribed to photoinduced free-carrier absorption (PFCA) [7]. The spectrum of sample C shows both characteristics of samples B and D; with respect to sample B the PA band is shifted toward higher energies. This data provides strong evidence for the existence of amorphous and crystalline phases in nanocrystalline samples.

This two-phase model is corroborated by the transient spectra. It was found [1] that the PM band of the amorphous phase in nc-Si:H has spectral features and time dependencies similar to those observed in a-Si:H [2,3], but with differences which can be understood as being due to increased disorder. Fig. 2 shows the decay of PFCA at 0.25eV as a function of delay time. The data can be described using stretched exponentials, which extend into much longer times than the exponential decays due to recombination in crystalline Si. They also show that the rate of recombination of free carriers in the crystalline phase is determined by recombination in the amorphous phase. The interpretation proposed in Ref. 1 assumes that the carriers generated in the grains have high mobilities and reach the grain boundaries very quickly, but only the holes become directly trapped in the amorphous phase. The electrons encounter a barrier in the conduction band due to the gap mismatch between the two phases and this prevents them from entering the higher lying conduction band or bandtail states in the amorphous phase. Thus, recombination is slower than in c-Si because the hole density in the grain has

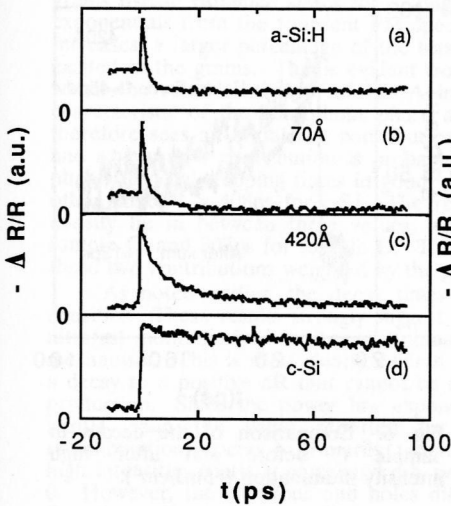


Fig. 3. Decays in photoinduced reflectivity $-\Delta R$ at 4.5 mJ/cm^2 pump intensity for four samples: a) a-Si:H; b) sample B; c) sample C; d) c-Si.

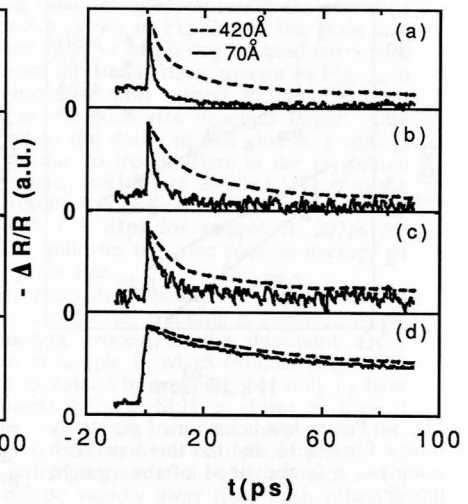


Fig. 4. Comparison of decays in ΔR for samples B (solid lines) and C (dashed lines) at four carrier densities (a) $N=7 \times 10^{20}$ (b) 3×10^{20} (c) 1×10^{20} (d) $2 \times 10^{18} \text{ cm}^{-3}$.

been reduced. The dominant recombination rate will be determined by how fast the electrons from the grain can reach a hole. Using this model and the transient decays measured in Ref. 1 one obtains stretched exponentials as in Fig. 2 which are consistent with the existence of amorphous and crystalline phases.

Results in the Picosecond Time Range

Previous studies [9,10] of a-Si:H and c-Si [10] under low intensity 2eV excitation ($\sim 10^{17} - 10^{18}$ carriers/cm³) have shown striking differences in the lifetime of carriers in extended states. Carriers in a-Si:H are trapped in low mobility states in tens of picoseconds, while those in c-Si live longer than a nanosecond. Recently, it has been found [11-13] that under high excitation conditions ($10^{20} - 10^{21}$ carriers/cm³) the lifetime of carriers in extended states for both of these materials is sharply reduced, coinciding with heat production on a picosecond time scale. In a-Si:H [11,12] the lifetime τ is approximately proportional to N^{-1} , whereas in c-Si [13] it is proportional to N^2 , where N is the density of photoexcited carriers. The former has been attributed to a fast nonradiative recombination of highly spatially correlated e-h pairs [14] due to either an Auger [11] or bimolecular [12] process. The latter is due to the normal Auger recombination. Since nc-Si:H may be viewed as a two-phase material, it is interesting to examine the picosecond trapping and recombination processes to determine under what conditions the amorphous or crystalline phase dominates on very short times scales.

Fig. 3 compares the transient decays in $-\Delta R$ for a-Si:H, c-Si, sample B and sample C under high illumination. The response in a-Si:H (Fig. 3a) is characterized by an initial decrease in reflectivity due to the excitation of free carriers by the pump pulse. This is followed by a subpicosecond decay to a constant positive value in ~ 10 ps. This decay is attributed to the nonradiative recombination of free carriers and subsequent production of heat [11,12], which

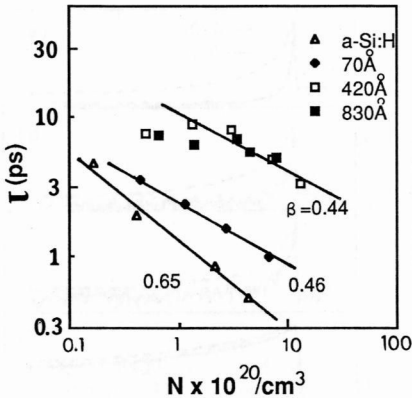


Fig. 5. Power law behavior of the decay time τ for a-Si:H and the three nc-Si:H samples. β is the slope of the straight line fits.

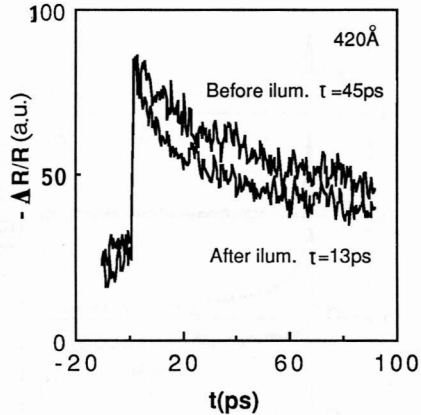


Fig. 6. Comparison of the decays in Sample C before and after high intensity illumination ($>5\text{mJ/cm}^2$).

causes a positive change in reflectivity. A similar behavior is observed in sample B, but the decay is somewhat slower, and ΔR decays to a less positive value than in a-Si:H. In sample C there is a fast decay component in the first 10ps followed by a much slower one over the duration of the trace, but no crossing of the zero line. The data in sample D are nearly identical to those on sample C, except for a slightly slower decay. In c-Si there is almost no decay on this time scale.

Further insight can be gained from Fig. 4, in which the decay curves for samples B and C are shown for a number of carrier densities between 10^{18} and $10^{21}/\text{cm}^3$. For all carrier densities $-\Delta R$ decays more slowly in the sample with the larger grain size. Moreover, for both samples the decays become faster with increasing carrier density. The data for sample B exhibit no positive ΔR below $2 \times 10^{20}/\text{cm}^3$ and are qualitatively similar to those of a-Si:H over the entire range of carrier densities studied. Finally, we note that for all the nc-Si:H samples there is a striking difference in the decay time between the data at high excitation densities ($>10^{19}/\text{cm}^3$) and those at low densities ($\sim 10^{18}/\text{cm}^3$). In Fig. 4a through 4c, both samples exhibit a rapid decay in $-\Delta R$ in the first 10ps; in Fig. 4d the decays are clearly much slower—on the order of hundreds of picoseconds. This indicates that we are in a different regime of carrier dynamics.

The data for all three grain sizes and a-Si:H were quantitatively analyzed by defining the decay time τ as the time at which $-\Delta R$ reaches half its initial value. Log-log plots of τ versus carrier density N for each sample are shown in Fig. 5. For a-Si:H, $\tau \propto N^{-\beta}$, where $\beta=0.65$. The data for samples B and C also exhibit power law behavior with exponent $\beta \approx 0.45$. It is important to note, however, that as the grain size increases one needs larger carrier densities to reproduce the same decay times and decay curves as are found in a-Si:H. In sample C, τ becomes insensitive to N below $10^{20}/\text{cm}^3$, and in sample D it is relatively independent of N except for the highest carrier densities studied.

Discussion

These observations lead us to suggest the following model to explain the data. At low intensities the carriers generated in the amorphous phase thermalize quickly ($<1\text{ps}$) and are trapped, while the electrons generated in the

grains live in extended states for a long time, in agreement with the stretched exponentials from the transient PM spectra shown in Fig. 2. As the grain size increases, a larger percentage of the total number of photogenerated carriers is excited in the grains. This is evident from the steady-state spectra in Fig. 1, in which the relative strength of PFCA increases with respect to the PM band characteristic of the amorphous phase as the grain size becomes larger. One therefore sees an initial fast contribution to the decay in ΔR due to trapping, and a very slow contribution is probably due to free carriers in the crystalline phase. Typical trapping times in good quality a-Si:H are 20-30ps [11]. On the other hand, $\tau = 408$ ps for c-Si. The results for nc-Si:H for the same carrier density lie in between these values, with $\tau = 81$ ps for sample B, 207ps for sample C, and 303ps for sample D. This indicates that one sees an average of these two contributions weighted by the grain size.

As noted earlier, the decay times drop dramatically for high excitation densities. These results strongly suggest that carrier trapping is replaced by an ultrafast nonradiative carrier recombination process as the dominant decay mechanism. This is most clearly evident in sample B, which exhibits (Fig. 4a,b) a decay to a positive ΔR that cannot be explained by trapping, but only by heat production. Since the power law exponent β for nc-Si:H is closer to that of a-Si:H than the value reported for c-Si [13], we conclude that this recombination process is primarily a characteristic of the amorphous phase. At high intensities spatially correlated e-h pairs are generated in both phases at $t = 0$. However, the electrons and holes diffuse rapidly away from each other as they thermalize in the crystalline phase, with the holes becoming trapped in the amorphous phase while the electrons remain behind in the grains. Therefore, only those carriers generated in the amorphous phase remain spatially correlated long enough to participate in a fast recombination process. It then follows that this process would be less efficient in nc-Si:H than in a-Si:H and would become even more so with increasing grain size. Sample C, for example, requires more carriers to obtain the same decay time measured in sample B because a greater percentage of carriers go into the crystalline phase, where they become ineffective in the recombination process. When the effective carrier density is rendered low enough, τ becomes nearly insensitive to the excitation density, as is exhibited in sample D and in sample C at intermediate intensities. It is surprising that $\beta < 1$ for all the samples measured. This indicates that the fast recombination process observed is not entirely the same as the one described in Refs. [11] and [14]. It is also clear that dispersive bimolecular recombination of trapped electrons and holes [15] is not applicable, since this would yield $\beta > 1$. In our case, the excitation densities under high illumination are large enough ($> 10^{20}/\text{cm}^3$) to saturate the shallow traps in the conduction band tail, thus indicating that at very short times (< 1 ps) we may be in a different regime of recombination kinetics than the one described in Ref. 15.

We have also found that the nc-Si:H samples are unstable under high illumination independent of grain size. Fig. 6 shows the decays in sample C at a given light intensity before and after the sample had been exposed to high illumination levels. The decay is more than three times as fast after the exposure. This is attributed to the creation of light-induced defects in the films, which increases the efficiency of the recombination process. Therefore all the measurements for this work were performed after the samples had been illuminated until they did not change anymore. It is important to note that under similar experimental conditions this effect was found to be negligible in a-Si:H.

In conclusion, steady-state and time-resolved spectral measurements have been performed which indicate that nc-Si:H can be described by a two-phase model with amorphous and crystalline phases. Ultrafast trapping and nonradiative recombination under high excitation conditions are primarily characteristics of the amorphous phase. It has also been shown that nc-Si:H is much more sensitive than a-Si:H to defect production under high illumination.

The authors thank T.R. Kirst for technical assistance. M.W. thanks IBM for a fellowship. This work was principally supported by NSF grant DMR

8706289.

References

1. Lingrong Chen, J. Tauc and Z. Vardeny, *Phys. Rev. B* **39**, 5121 (1989).
2. H.A. Stoddart, Ph.D. Thesis, Brown University, 1987.
3. H.A. Stoddart, Z. Vardeny and J. Tauc, *Phys. Rev. B* **38**, 1362 (1988).
4. H.T. Grahn, C. Thomsen and J. Tauc, *Opt. Commun.* **58**, 226 (1986).
5. R.L. Fork, B.I. Greene and C.V. Shank, *Appl. Phys. Lett.* **38**, 671 (1981).
6. W.H. Knox, M.C. Downer, R.L. Fork and C.V. Shank, *Opt. Lett.* **9**, 552 (1984).
7. Hsiang-na Liu, D. Pfost and J. Tauc, *Sol. State Commun.* **50**, 987 (1984).
8. Z. Vardeny, T.X. Zhou, H. Stoddart and J. Tauc, *Sol. State Commun.* **65**, 1049 (1988).
9. Z. Vardeny and J. Tauc, in *Disordered Semiconductors*, eds. M.A. Kastner et al., (Plenum Press, N.Y., 1987) p. 339.
10. J. Kuhl, E.O. Gobel, Th. Pfeifer and A. Jonietz, *Appl. Phys. A* **34**, 105 (1984).
11. A. Esser, K. Seibert, H. Kurz, G.N. Parsons, C. Wang, B.N. Davidson, G. Lucovsky and R.J. Nemanich, Proceedings of the 13th International Conference on Amorphous and Liquid Semiconductors, *J. Noncryst. Sol.* (to be published).
12. A. Mourchid, D. Hulin, C. Tanguy, R. Vanderhagen and P.M. Fauchet, Proceedings of the 13th International Conference on Amorphous and Liquid Semiconductors, *J. Noncryst. Sol.* (to be published).
13. M.C. Downer and C.V. Shank, *Phys. Rev. Lett.* **56**, 761 (1986).
14. W. Rehm and R. Fischer, *Phys. Stat. Sol. (b)* **94**, 595 (1979).
15. J. Orenstein and M.A. Kastner, *Sol. State Commun.* **40**, 85 (1981).